Tomas Sanches[1], Nadir Yilmaz[2], Walt Gill[3], and A.B. Donaldson[3]

[1]*Omicron Inc., Albuquerque, NM*
[2]*New Mexico Institute of Mining and Technology, Socorro, NM*
[3]*Sandia National Laboratories, Albuquerque, NM*

Abstract

Accidents involving solid propellant containing aluminum can be difficult to model due to the unknown contribution produced by molten aluminum or alumina impingement/deposition on target objects. A series of tests has been carried out using a commercially available oxy-acetylene torch and powder feeder to investigate the affects of molten/oxidized aluminum on stainless steel 304 substrates. For some tests, the stainless steel substrate was heated with torch gases to an elevated temperature before aluminum powder injection. SEM and EDS have been used to determine diffusion/reaction of aluminum into the stainless steel and characterize the constituents of the resulting interfacial layers. SEM and EDS analysis indicated that at the test conditions, aluminum was undetectably oxidized before it deposited on the substrate surface. However, temperature data from thermocouples attached to backside of each substrate detected a significant increase in heat flux to the substrate when aluminum is introduced into the torch combustion gases. Results also indicate that the interface between the aluminum and stainless steel were well defined implying that little diffusion or solution of the aluminum with the stainless steel has occurred.

Further, a series of tests examined the amount of aluminum that is collected on a surface located directly below an upward burning sample of solid propellant above the surface. The collected aluminum/alumina is similar in composition to that from the torch. Of further interest, the amount of aluminum recovered from the solid propellant burns was inversely proportional to the diameter of propellant.

Introduction

Aluminum powder is typically added to solid propellant used in rocket propulsion motors to enhance the burning characteristics of the solid propellant. However, accidents could cause the solid propellant to ignite and burn in undesirable situations and expose high risk payloads to a severe thermal environment. A solid propellant fire can be considered a more complicated scenario than a typical hydrocarbon fuel fire partly due to the unknown oxidation state of aluminum and aluminum/alumina particle impingement/attachment to surrounding objects. The heat transferred to the surrounding objects as a result of the aluminum contribution is difficult to predict as current fire models are only now attempting to account for impingement/attachment.

Aluminum itself has been the subject of much research regarding its ignition characteristics which are currently not well understood, and the extent to which aluminum/products attach to a target and gives up either latent heat or the aluminum enthalpy of combustion. These two aspects of aluminum encompass the major objectives of this experiment. The primary focus of this experiment is characterizing the aluminum and stainless steel interface when molten/oxidized aluminum is sprayed on a stainless steel substrate using an oxy-acetylene torch. Some research regarding heated particles impinging a substrate focus on understanding the mechanism that bonds the particles to the substrate in hopes of understanding adhesion.

Kitahara and Hasui [1] were one of the first to describe the inter-metallic processes associated with coating deposition on substrate materials. Using a scanning electron microscope (SEM), they observed the sprayed particles melt the substrate surface layer and amalgamate. McPherson [2] concentrated on understanding individual particle/substrate interactions and suggested that the real contact area between the particle and substrate is less than the apparent area because of absorbed and entrapped gas, oxide films or other contamination. Contaminates tend to adversely affect the adhesion of the particles to the substrate.

In addition to the torch tests, an effort was made to determine the composition of the aluminum deposit from solid propellant. It has been observed that a significant amount of aluminum/alumina is deposited on surrounding objects during ambient burning of the propellant. The quantity and composition of the deposit will further validate the use of the torch in simulating solid propellant burns. A rough estimate was also made, based on the amount of aluminum recovered, as to how much aluminum was converted to alumina.

In summary, for the work which is reported here, the objective to understand how the parameters which can be varied with the torch/aluminum powder feed, will influence the state of aluminum and its adhesion to a stainless steel plate which can be preheated to various temperatures before the powder feeder is activated. However, some side work included temperature measurements and composition of deposit of aluminized solid propellant.

Experiment Setup

Thermal Spray

A commercially available torch (Sulzer Metco 6P-II) and a Hardface Alloy, Inc. Hopper (model HA500F-SA) were used to simulate a small propellant fire. The torch was designed to flame spray coatings on various surfaces by heating powder feed stock using an oxy-fuel flame. A hopper, in conjunction with an inert carrier gas, is used to evenly supply powder feed stock to the torch. The torch was mounted vertically on an optics table and placed directly beneath an overhead exhaust hood. A simple stand, used to hold the stainless steel substrate above the torch, was also attached to the optics table. Figure 1 is a diagram of the basic experiment setup.

The torch is capable of numerous hardware configurations that vastly affect the flame temperature, particle temperature, and particle velocity. Urrea *et. al.* [3] performed a series of tests that characterized these parameters using the Sulzer Metco 6P torch and a powder hopper. The results showed that the highest flame and particle temperatures are achieved using nozzles that inject powder directly into the flame jets. For this reason, the torch was fitted with a type-D nozzle (Sulzer Metco, Westbury, NY) and a gun cooling air cap.

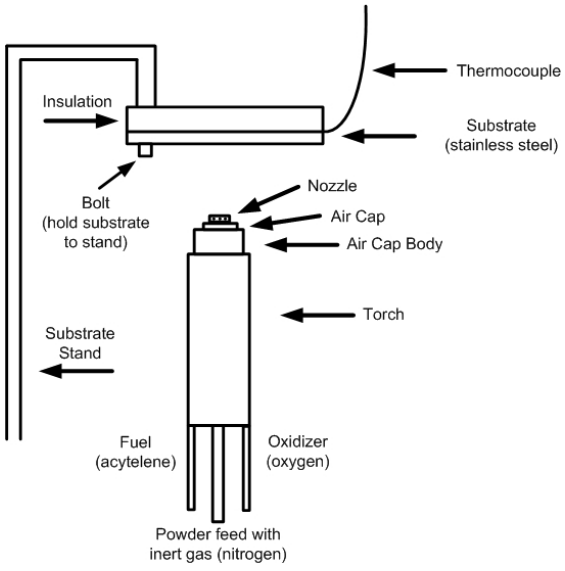

Figure 1. Experiment setup

Stainless steel 304 plates approximately 4 in. x 4 in. x 3/32 in., were used as the substrate for the various tests. Each plate had an intrinsic type K thermocouple affixed to the backside. A stainless steel strap was tack welded

around the thermocouple lead wires to provide strain relief. A single stainless steel screw was used, in conjunction with a small hole in the corner of the plate, to fix the plate to the stand.

The purpose of this series of test was to cause as much degradation to the substrate as possible using elevated temperature and exposure to the powder aluminum and any oxidation products. This was performed by varying the powder size, powder feed rate, and separation distance between the plate and the torch nozzle. Table 1 presents the specific parameters of each test.

Table 1. Test matrix

	Test Parameters							
	1	**2**	**3**	**4**	**5**	**6**	**7**	**8**
Powder Size [μm]	95	95	95	30	30	30	30	30
Powder Feed Rate* [rpm]	138	138	138	700	500	300 w/ramp to 500	500	500
Separation Distance [in.]	3	3	6	3	1.5	1.5	1.5	1.5
Substrate temperature before powder [°C]	850	1038	725	1020	†	†	††	†
Insulation	Present	Present	Present	Present	Present	Absent	Absent	Absent

† The thermocouple temperature range was exceeded before introducing aluminum powder.
†† No thermocouple was attached.

After each test case, the plate was allowed to cool and then placed in a plastic bag to prevent any contamination of the sample. The plates were then prepped for further analysis, specifically: sectioned, potted, polished and then, studied by SEM and energy dispersive spectrometry (EDS).

Solid Propellant Burns

Solid propellant samples consisting of approximately 68% ammonium perchlorate (AP), 19% aluminum, 9% hydroxy-terminated polybutadiene, and 2% placticizer (DOA) were allowed to burn freely. The samples were cylindrical with diameters of 5, 6, 12, and 18 inch (12.7, 15.24, 30.48, and 45.72 cm) with a common height of 1.7 inches (4.32 cm). Each sample was inhibited to burn in planar fashion. During the propellant experiments, the deposits were gathered after each burn. The deposits, comprised of fine-powder to large metallic chunks, were then weighed. Random pieces and a few grains of powder of Test M-14 were further analyzed using scanning electron microscope (SEM) and energy dispersive spectra (EDS) to determine the deposit's composition. It is important to note that the composition could only be roughly approximated as oxygen x-rays are absorbed by the beryllium window and oxygen is more susceptible to an activation energy of 5 kV instead of the 15 kV used for aluminum.

The EDS results were used to derive the fraction of the deposit that is alumina (Al_2O_3). This required a major assumption based on the past experience of personnel that have observed EDS data of reagent grade alumina powder. EDS results of reagent grade alumina indicated that the amount of oxygen observed is 50% that of aluminum. Therefore, a correction factor is applied to the fraction of the sample that is alumina. The correction factor for aluminum is expressed as

$$\left(\frac{x\%Al_2O_3}{y\frac{O}{Al}}\right)_{deposit} = \left(\frac{100\%Al_2O_3}{0.5\frac{O}{Al}}\right)_{pure Al_2O_3} \quad (1)$$

where, x = percentage of alumina in deposit

y = ratio of oxygen to aluminum in deposit

The ratio of oxygen to aluminum in the deposit, y, is determined from an average of the EDS data.

Results and Discussion

SEM and EDS analysis

SEM and EDS were used to investigate the interface of the aluminum powder and the stainless steel substrate. The plates were prepared for analysis by first potting them in a carbon epoxy that contains a small amount cholride. Next, excess material, material far from the center line of the plate, is trimmed away. A final cut perpendicular to the powder/substrate interface creates the surface of interest. The exposed surface of each sample's stainless steel plate and aluminum was polished, thus finishing the sample preparation.

SEM analysis has been used to take high-magnification, high-resolution images of the samples. Magnification ranged from 55 to 3,000X. The images produced from the SEM provide significant information that highlights the mixing layers of the substrate and particulate and the associated porosity within those layers. Figure 2 and Figure 3 are SEM images at 55 and 2,000 X, respectively.

The light gray portions towards the bottom of Figure 2 and Figure 3 correspond to stainless steel 304 that did not interact with the sprayed aluminum. The dark gray regions of the figures correspond to aluminum. The shades of gray between the light and dark represent the various mixing layers of aluminum and stainless steel. Porosity of the sprayed aluminum is evident by the black portions of the figures, which corresponds to the potting material which filled in the voids.

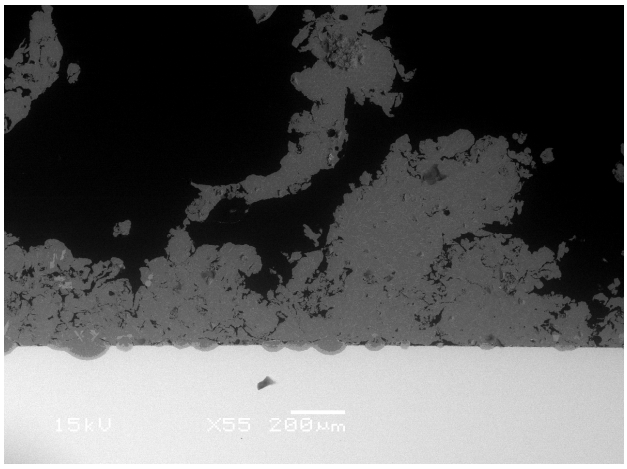

Figure 2. SEM image at 55X.

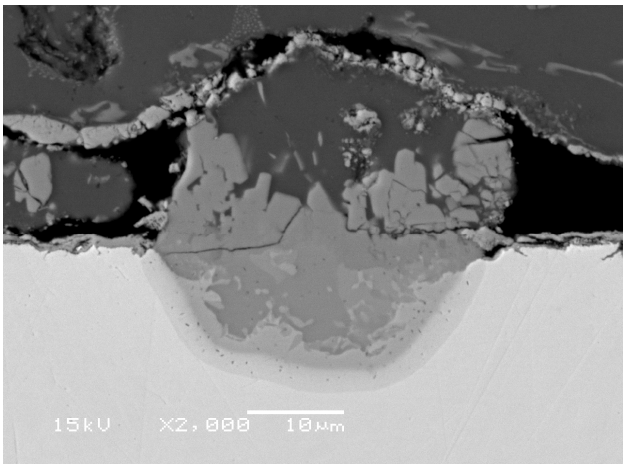

Figure 3. SEM image at 2,000X

The high magnification permitted specific target points and areas on the sample to be analyzed with EDS. The function of EDS is to identify elements at a specific location within the sample. Typically, the analyst chose

points or areas traversing the aluminum/stainless steel interface to determine the extent of aluminum particle penetration into the stainless steel substrate and the composition of the resulting alloy layers.

EDS was initially performed on all samples using a low vacuum chamber and no surface coating. However, the low vacuum chamber contained enough air that the electron beam from the SEM/EDS was unable to focus a true point at the sample's surface. Further, the lack of conductive coatings on the samples led to the buildup of a surface charge on the samples. The combined effects of the ambient air in the chamber and the buildup of a surface charge caused the SEM/EDS electron beam to sample a halo around the target point. These effects became evident when portions of the plates that were expected to be stainless steel instead showed significant concentrations of aluminum.

Improved EDS data was accomplished by applying a very thin coat of gold to the surface of the sample and evacuating the chamber until high vacuum was reached. The gold coating improved the grounding of the sample and prevented the surface from building up a charge. A high vacuum chamber permitted the electron beam to focus on a tight point.

Please note that due to the amount of data recorded, the following images and EDS plots are presented below for Test 1 only.

Results for Test 1

The parameters selected for this test produced little deformation of the stainless steel substrate as evidenced by Figure 4 and 6. A small amount of aluminum deposition is visible in Figure 4, as well as soot produced during shutdown of the torch. Figure 6 is a photo of sample 1 as prepped for SEM/EDS analysis. The opaque material surrounding the shiny metallic sample is a carbon epoxy that stabilizes the sample.

Figure 7Figure 8 illustrate the stainless steel substrate and aluminum powder interface at low and high magnifications, respectfully. Individual aluminum particle penetration into the stainless steel substrate is apparent in both of the figures. EDS data for sample 1 was taken at the seven points which is shown in Figure 9.

Figure 4. Test 1 bottom

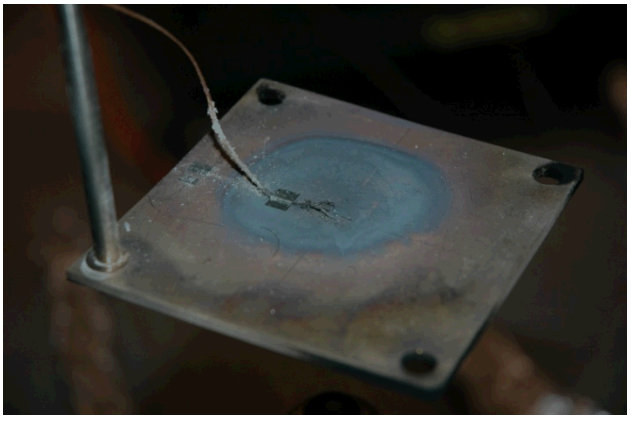

Figure 5. Test 1 top

Figure 6. Test 1 prepped for SEM/EDS analysis

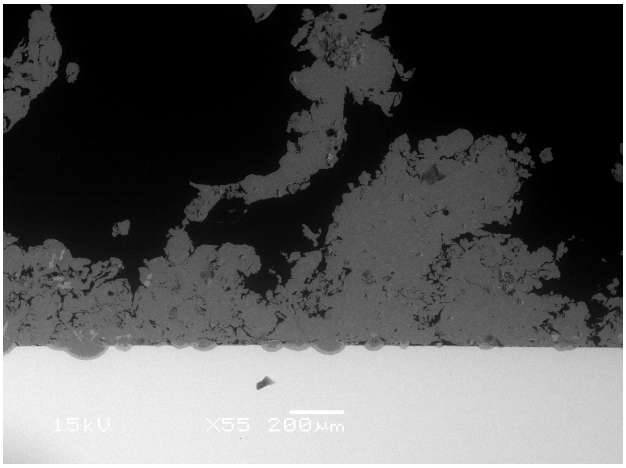

Figure 7. Test 1 low magnification image

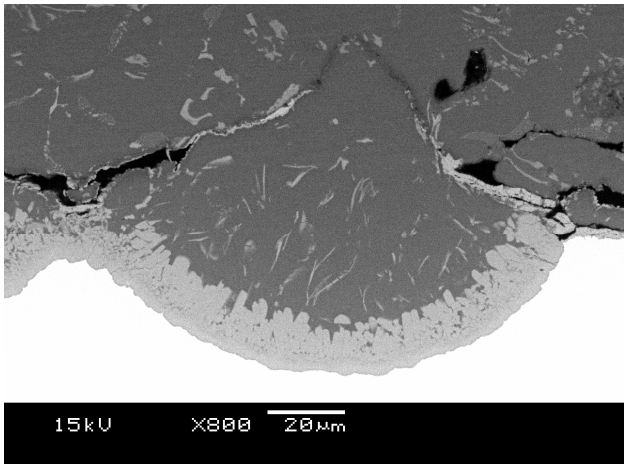

Figure 8. Test 1 medium magnification image

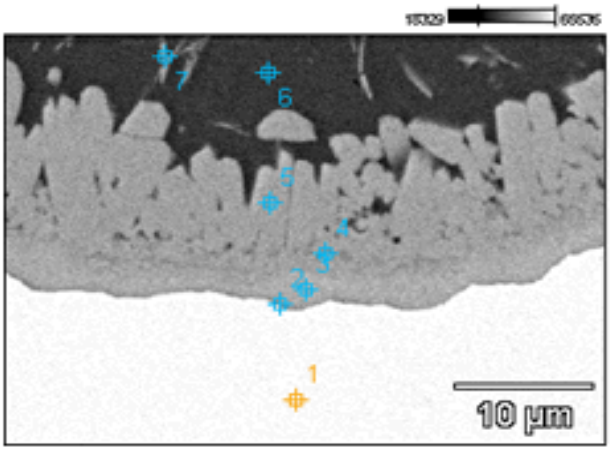

Figure 9. Test 1 EDS sample points. Corresponding spectra shown in Figures 11-17.

The following plots present the spectra for each of the seven points shown in Figure 9. It is assumed that any gold or manganese peaks present in the spectra originated from the gold coating. Manganese and gold share some spectra peaks.

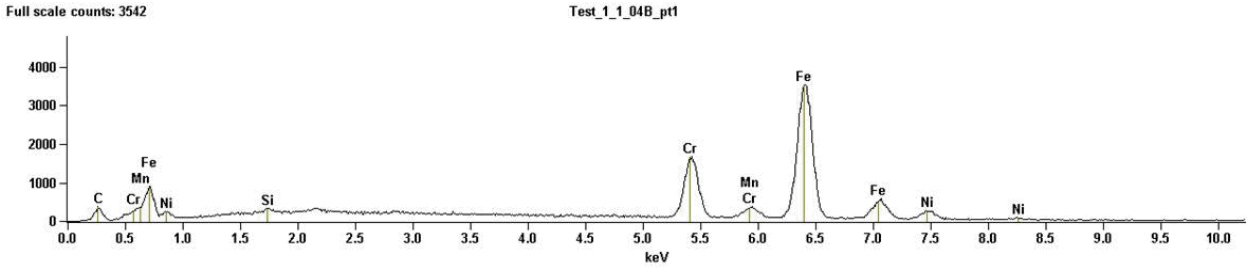

Figure 10. EDS spectra for point 1 of Test 1

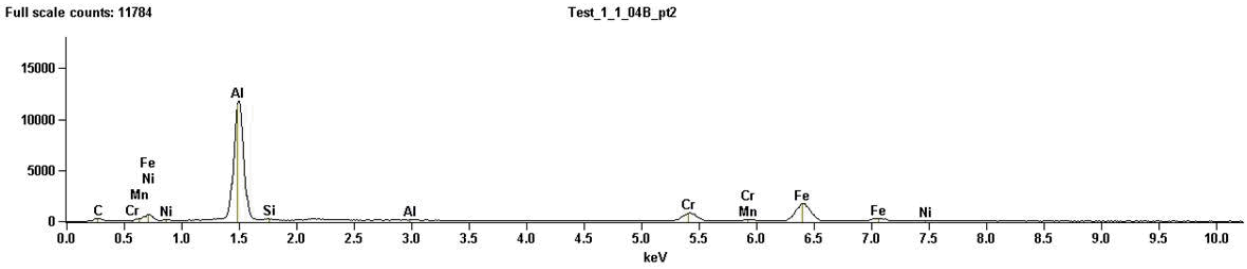

Figure 11. EDS spectra for point 2 of Test 1

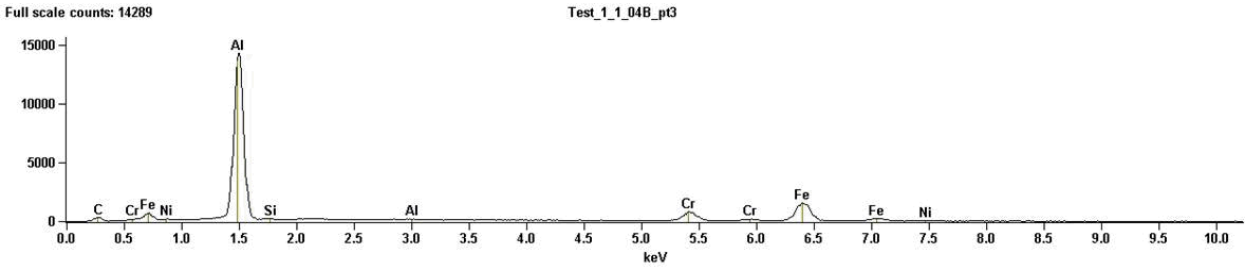

Figure 12. EDS spectra for point 3 of Test 1

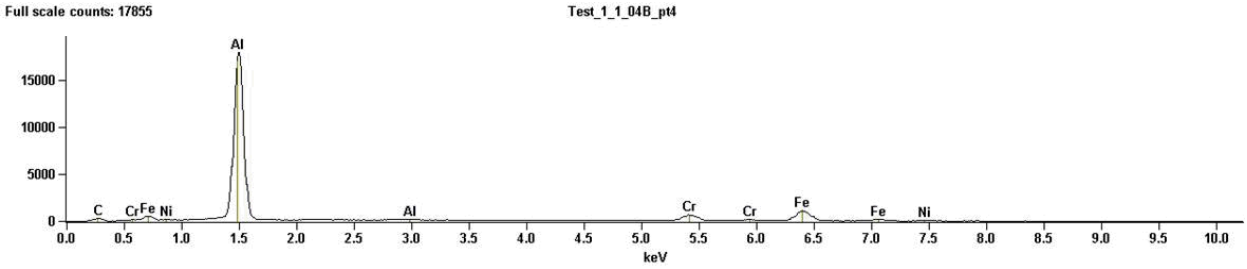

Figure 13. EDS spectra for point 4 of Test 1

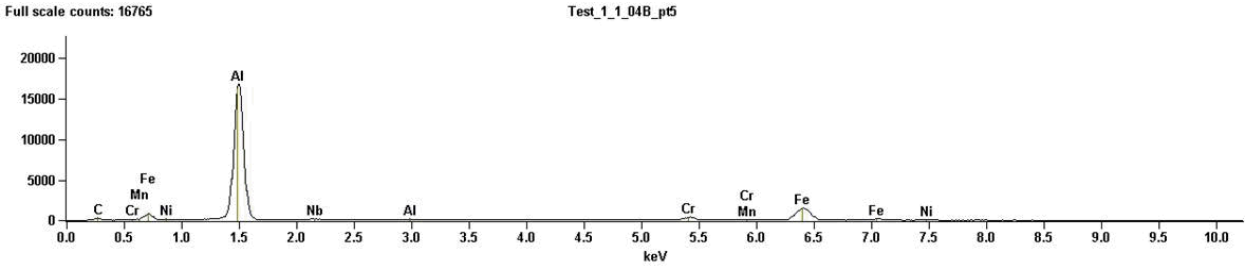

Figure 14. EDS spectra for point 5 of Test 1

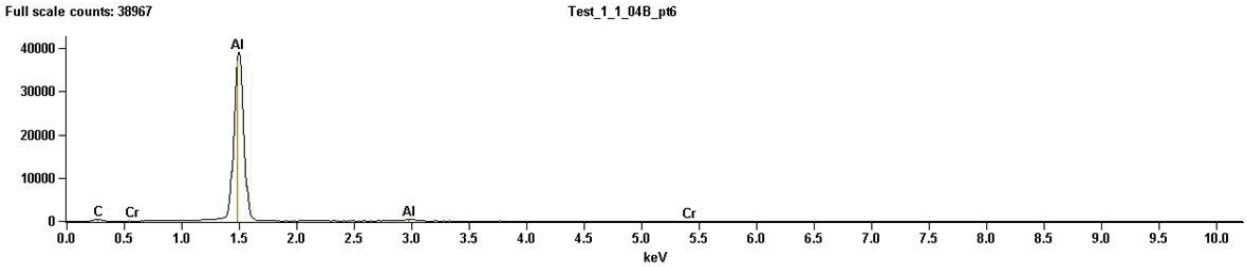

Figure 15. EDS spectra for point 6 of Test 1

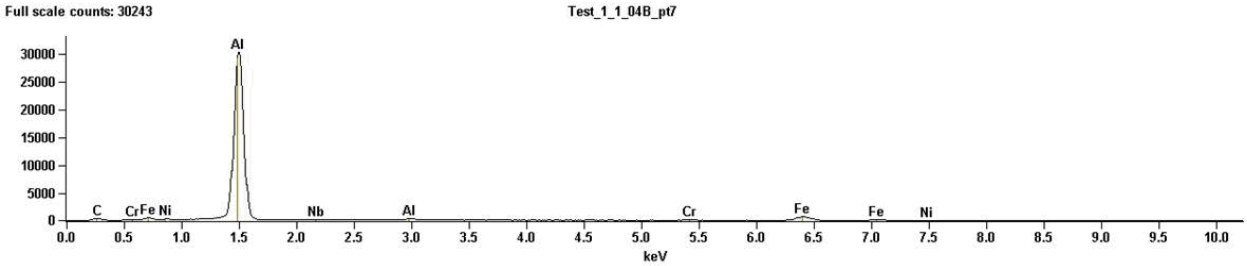

Figure 16. EDS spectra for point 7 of Test 1

Figure 9 clearly shows that point 1 is in a region that is expected to be stainless steel 304. This is confirmed as the spectra in Figure 10 shows no aluminum peaks. Stainless steel 304 contains approximately 70% iron, 18-20% chromium, 8-10% nickel, and small amounts of carbon, manganese, silicon, phosphorus, sulfur, and nitrogen [Ref. 4]. The major constituents of stainless steel are present in the spectra shown in Figure 10.

The spectra for point 2, as seen in Figure 11, shows a spike in the amount of aluminum present. Based on the SEM image, point 2 corresponds to the farthest point that one would expect to see aluminum penetration/diffusion. However, the spectra also indicates a significant drop in the presence of stainless steel. This implies that the boundary layer between the aluminum and stainless steel is rather small in comparison to the thickness of the stainless steel plate and no significant solution is occurring that would compromise the structural integrity of the substrate. It is important to note that this does not imply that structural integrity of the substrate is intact as the flame temperatures produced by the torch significantly exceed the melting temperature of stainless steel.

Points 2 through 5 essentially reside in the same region. Figure 11 through 15 confirm the spectra for the four points are nearly identical. Virtually no stainless steel is present in points 6 and 7 as seen in Figure 15 and 17.

EDS for points 6 and 7 also indicate that there is no oxygen present. This implies that little alumina is present within the deposit. White [Ref. 5] also noted the lack of oxygen in the spectra of an experiment similar to the test reported here. It was originally thought that more oxidized alumina would be present in the deposit.

Regardless of the oxidation state of alumina, the aluminum powder causes a significant increase in heat flux to the substrate. This observation is evident in Figures 18-24 and was also noted in reference 5.

Thermocouple Data for Tests 1-8

Thermocouple data for most data samples were recorded. The data obtained by the thermocouple provides significant insight on the effects of the aluminum as it is deposited on the stainless steel substrate. The following figures are plots of the temperature for each test with attached thermocouples.

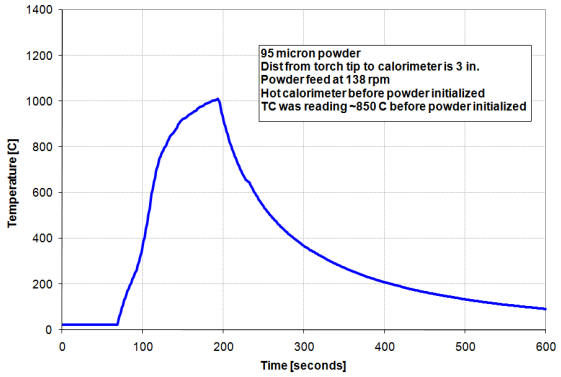

Figure 17. Test 1 thermocouple data

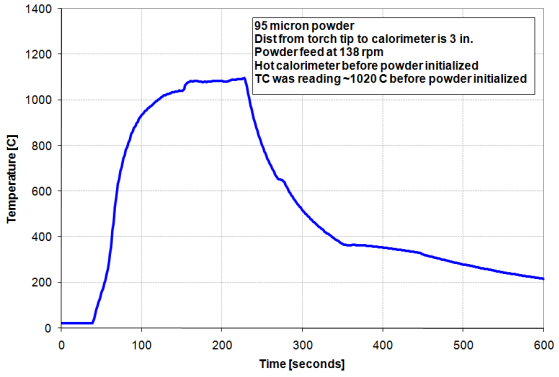

Figure 18. Test 2 thermocouple data

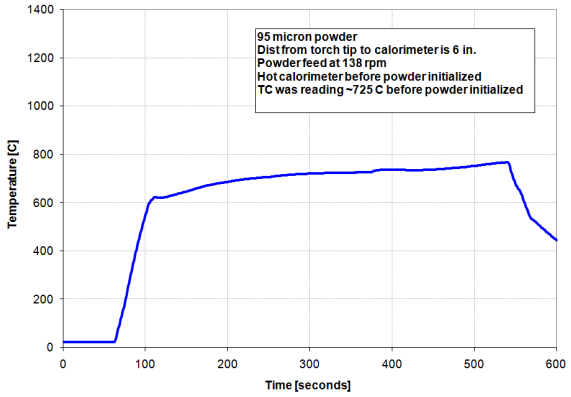

Figure 19. Test 3 thermocouple data

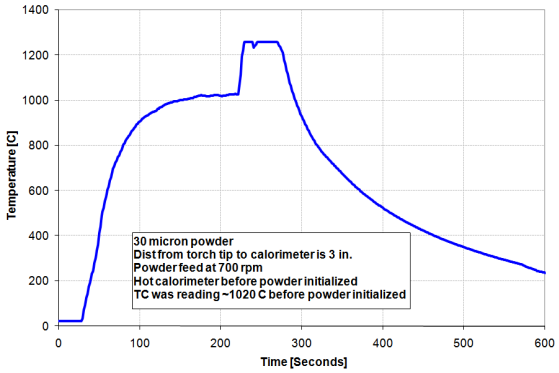

Figure 20. Test 4 thermocouple data. Flat top indicates that thermocouple limits were exceeded.

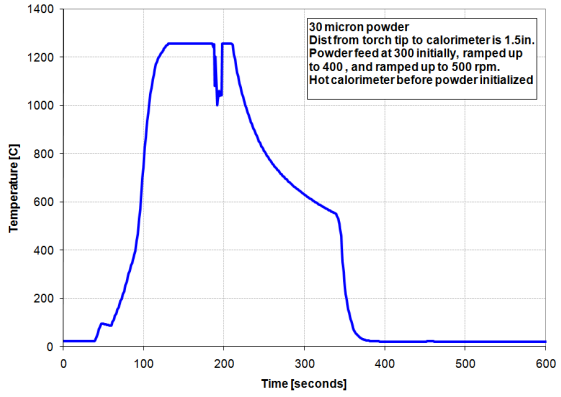

Figure 21. Test 5 thermocouple data. Flat top indicates that thermocouple limits were exceeded.

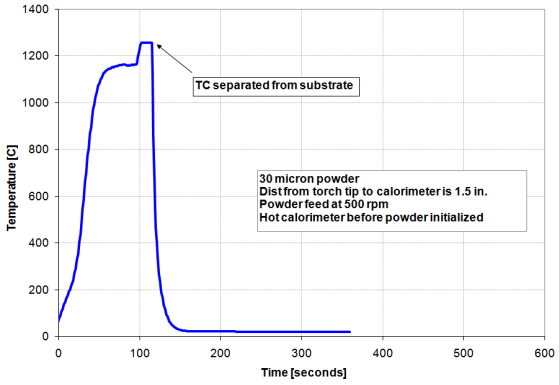

Figure 22. Figure 6 test data

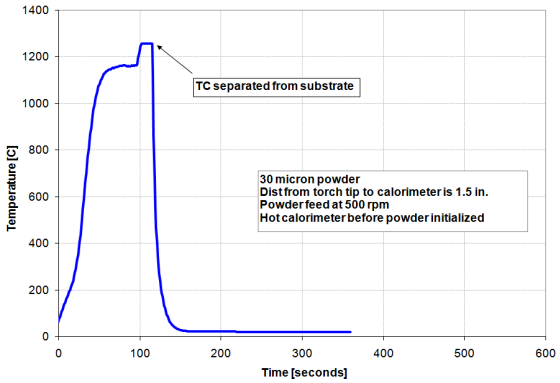

Figure 23. Test 8 thermocouple data

The thermocouple data agrees with the observations of White [Ref. 5] in that introducing the aluminum powder increases the heat flux to the target. This phenomenon is especially clear in tests where the substrate was preheated. Specifically, tests 2, 4, and 6 have temperature histories that begin to flatten after the initial rise and then a sudden increase in temperature occurs. However, the distance to between the substrate and torch proved to be the dominating factor in affecting temperatures.

Several flat spots in the data are observed around 1260 ºC. At this temperature the data acquisition system has reached the limits of the type K thermocouple range. The thermocouple will continue to produce a voltage differential with respect to reference junction and if the temperature drops within the type K range, the data acquisition will continue to record temperatures. However, at excessive temperatures, the thermal damage to the substrates was sufficient enough to separate the tack welds that held the thermocouple leads and strain relief strap.

Solid Propellant Deposit and Composition

To determine how much aluminum was in each sample, the sample weight was multiplied by the aluminum wt. %. The aluminum comprises 18-20 wt.% of the Areojet/Atlas-V solid propellant. For the purpose of this paper, it is assumed that the aluminum is 19 wt.%. No recovered aluminum was provided for tests M-11, M-13, or M-15. Test M-5R was more than likely mismarked as the deposit weighed more than the initial amount of aluminum. The amount of deposit recovered from Test M-5R suggests that it was a 12 in. diameter burn.

The results and pictures of the SEM and EDS data are presented below.

Table 2. Summary of recovered deposits

Test ID	Initial Sample Weight			Recovered Powder [g]	Recovered Solid [g]	Total Deposit Recovered [g]
	diameter [in.]	Propellant Mass [g]	Mass of Al [g]			
M-5	5	988.0	187.7	31.6	89.4	121
M-6	5	988.0	187.7	39.5	93.5	133
M-7	12	13706.4	2604.2	176.7	1415	1591.7
M-8	12	13706.4	2604.2	188.7	1528.7	1717.4
M-9	18	30128.2	5724.4	-	3132.6	3132.6
M-10	18	30128.2	5724.4	-	3175	3175
M-12	6	3347.6	636.0	133.2	358.6	491.8
M-14	12	13706.4	2604.2	156	1457.3	1613.3
M-16	18	30128.2	5724.4	-	2521.8	2521.8

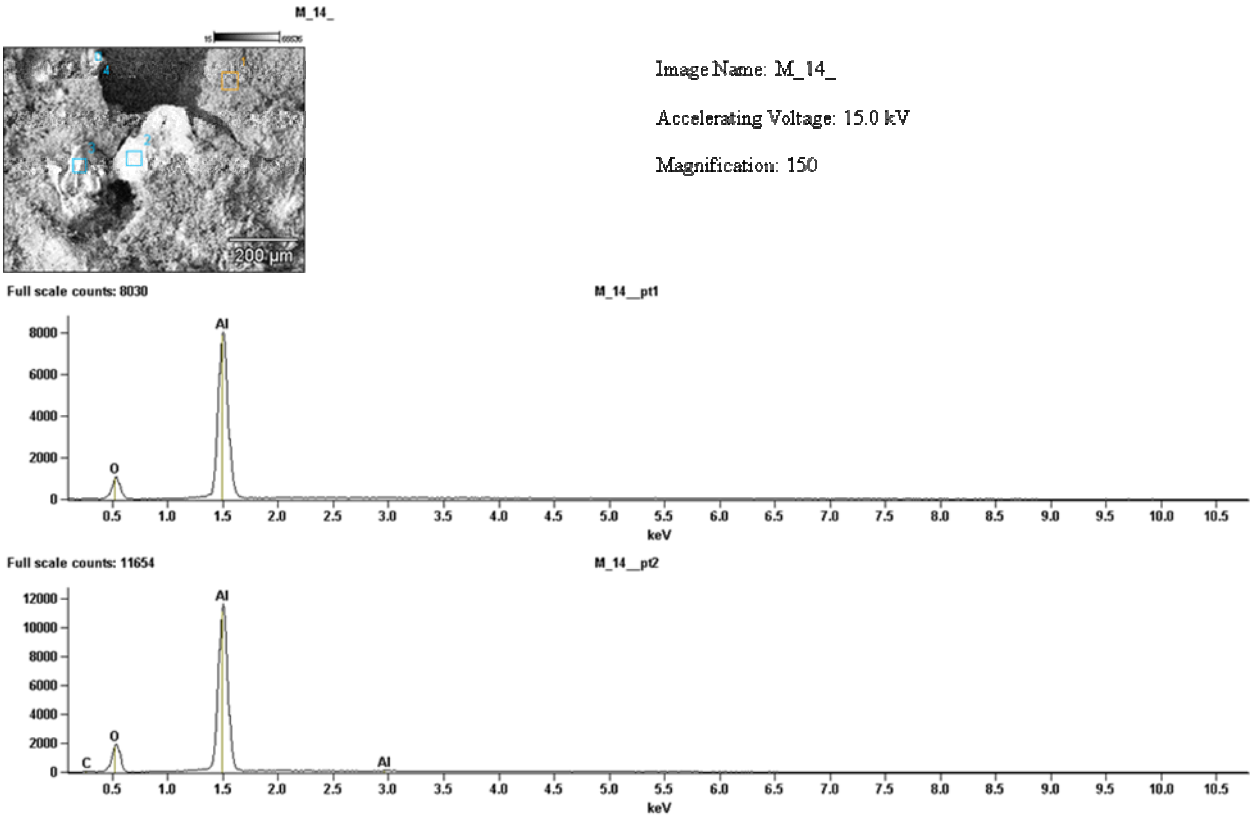

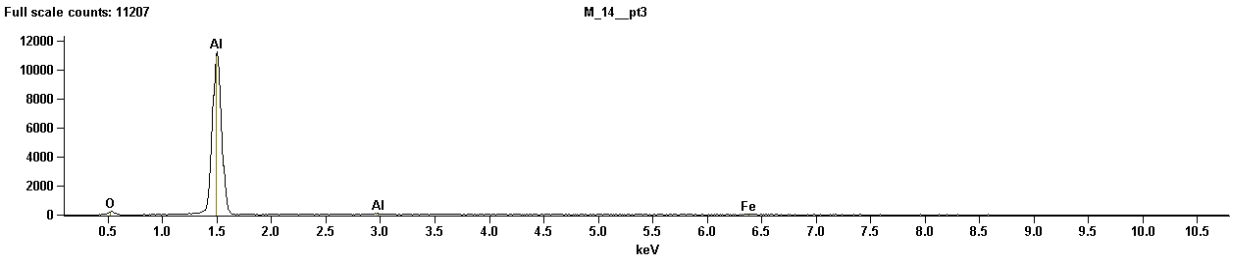

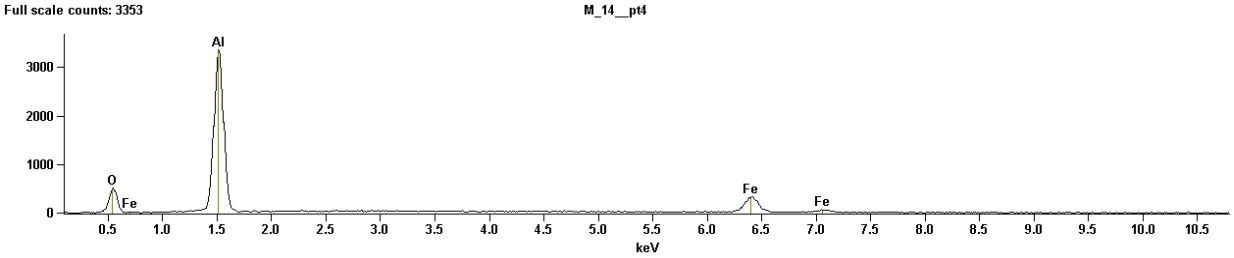

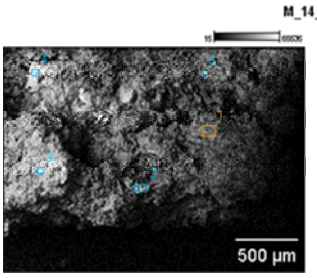

Image Name: M_14_02B

Accelerating Voltage: 15.0 kV

Magnification: 55

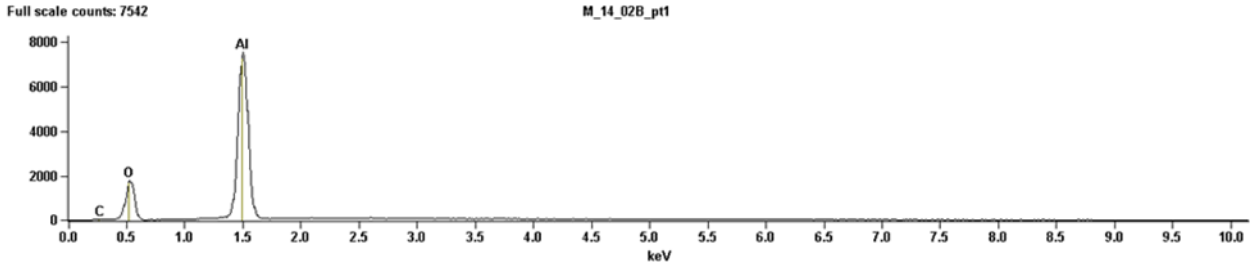

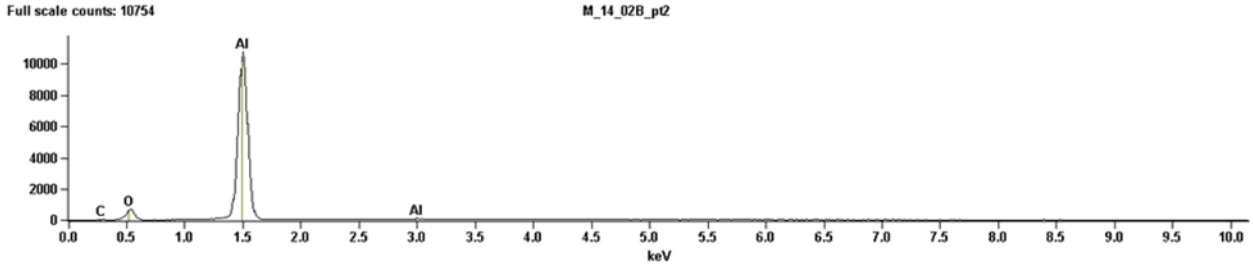

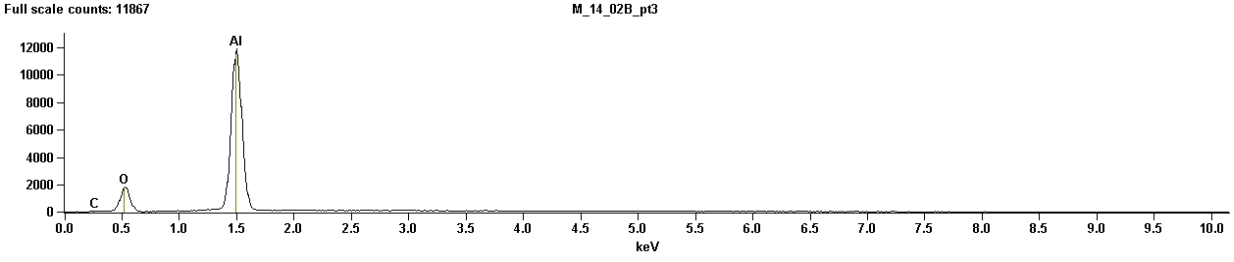

Full scale counts: 13283

M_14_02B_pt4

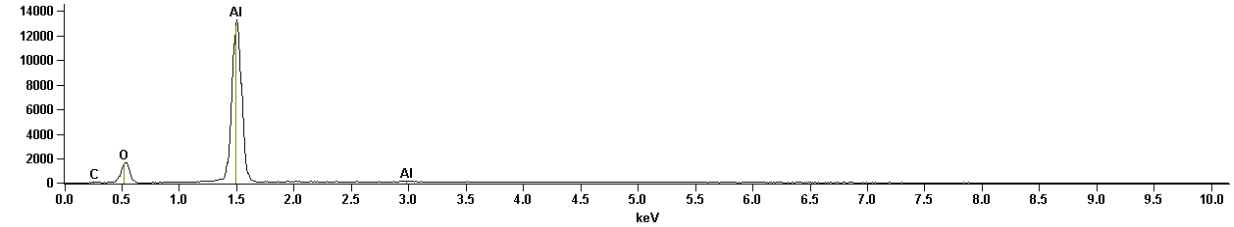

Full scale counts: 9374

M_14_02B_pt5

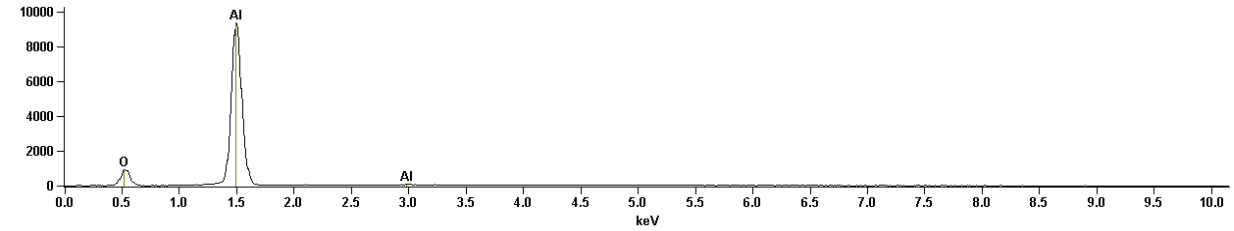

M_14_03B

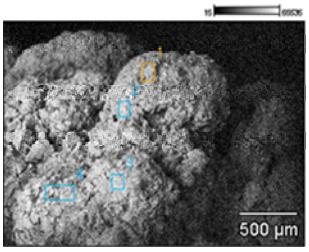

Image Name: M_14_03B

Accelerating Voltage: 15.0 kV

Magnification: 50

Full scale counts: 9176

M_14_03B_pt1

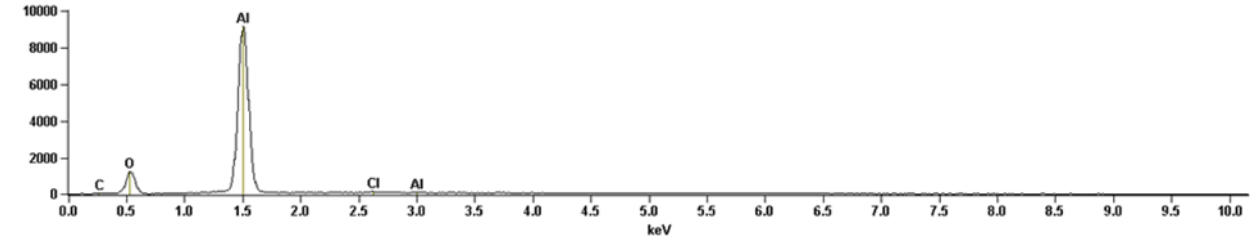

Full scale counts: 12788

M_14_03B_pt2

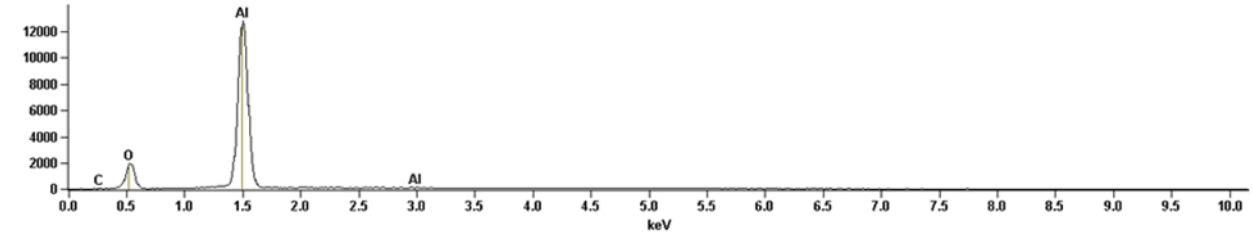

Full scale counts: 12859

M_14_03B_pt3

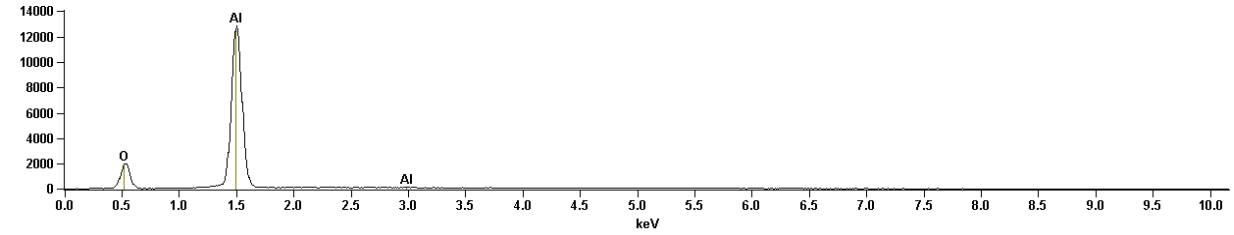

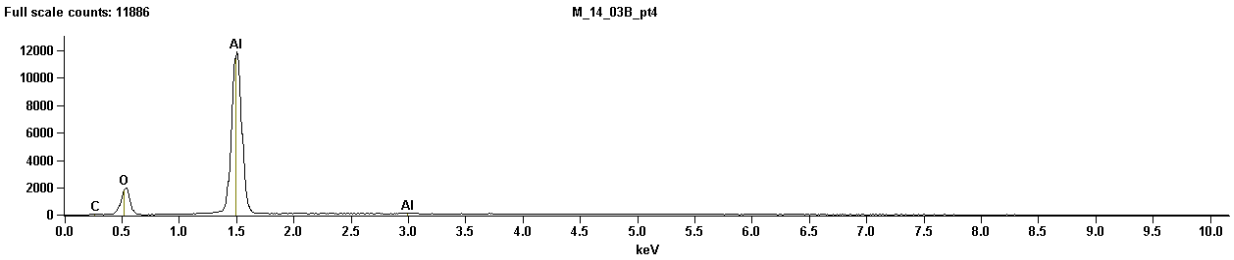

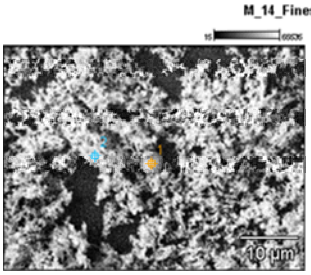

Image Name: M_14_Fines_M14F_01B

Accelerating Voltage: 15.0 kV

Magnification: 2500

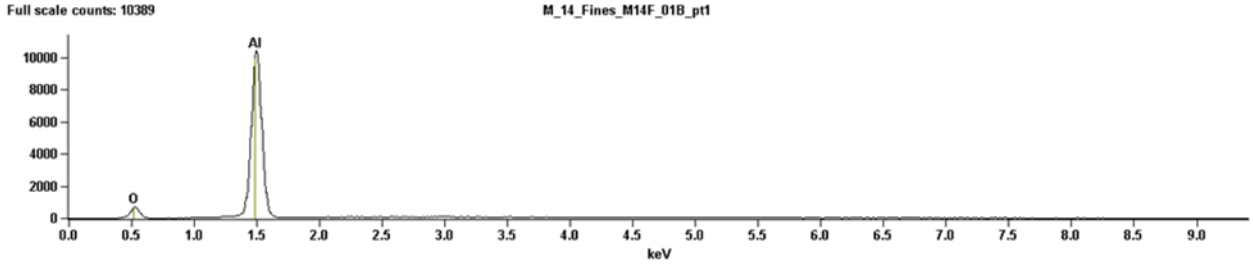

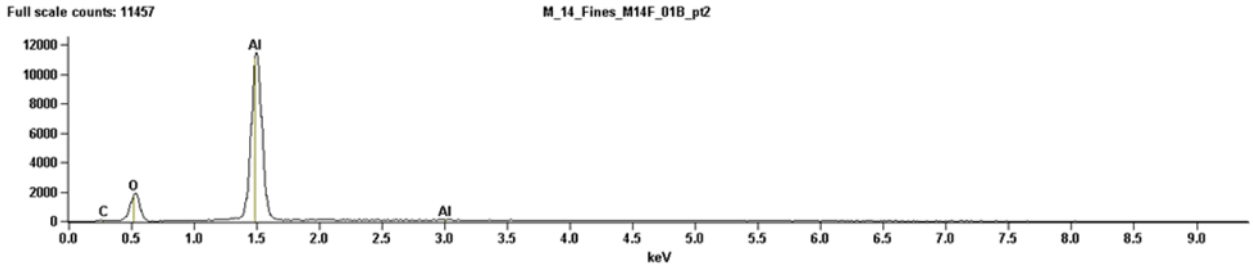

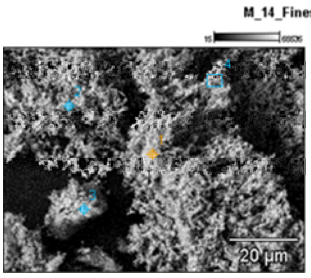

Image Name: M_14_Fines_M14F_02B

Accelerating Voltage: 15.0 kV

Magnification: 1500

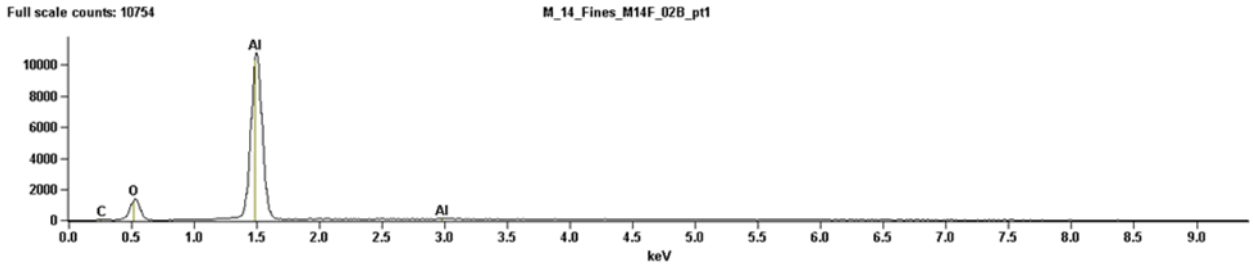

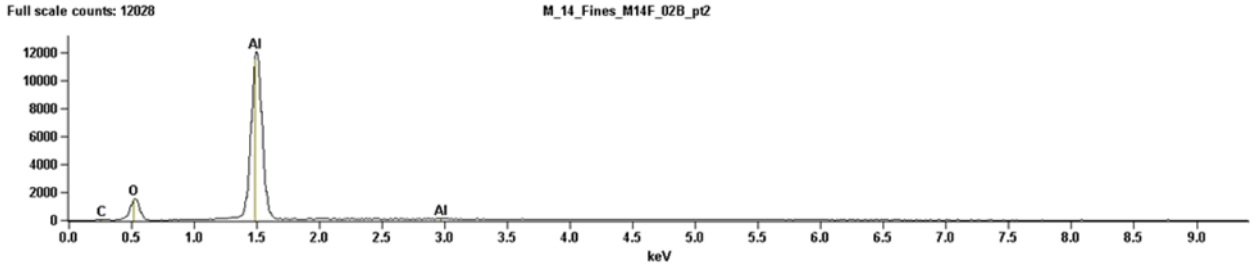

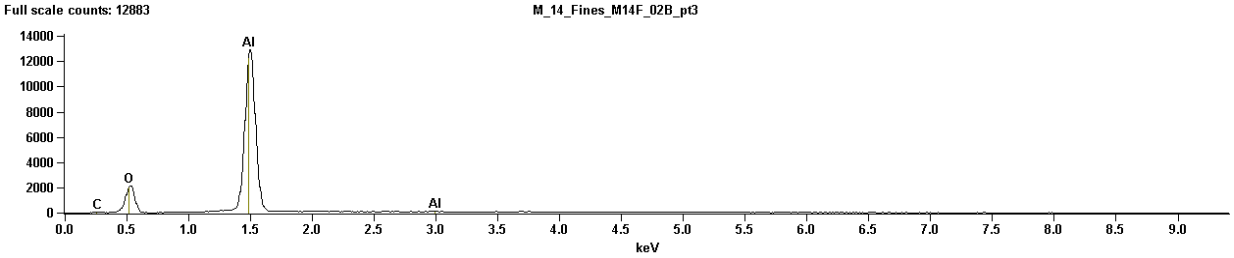

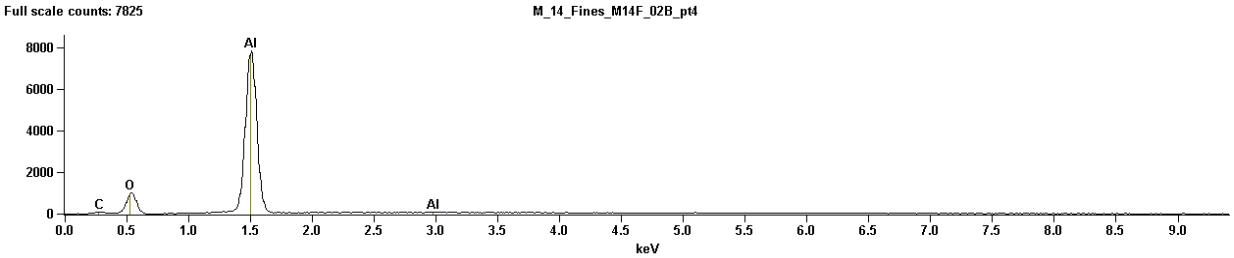

The above EDS plots are summarized in the following table. Only the counts for oxygen, 0.5 keV, and the first aluminum peaks, 1.5 keV are tracked.

Table 3. Oxygen and aluminum counts from EDS

Oxygen	Aluminum	Oxygen	Aluminum
1200	8000	2000	12000
2000	12000	2000	14000
500	12000	2000	12000
500	3500	1000	10000
2000	8000	2000	120000
1000	11000	2000	10000
2000	12000	2000	12000
2000	14000	2000	14000
1000	10000	1000	8000
1500	9500	-	-

Average number of counts for oxygen and aluminum are 1600 and 16000, respectfully. This implies that oxygen percentage, *y,* is

$$y = \frac{1600}{16000} = 10\% \tag{2}$$

Rearranging equation 1 and solving for the unknown Al_2O_3 % gives

$$x = 10\%\left(\frac{100\% Al_2O_3}{0.5}\right)_{pure Al_2O_3} \tag{3}$$

$$x = 20\% Al_2O_3 \tag{4}$$

Based on the methodology and assumptions, it appears the deposit is approximately 20% on a molar basis. To determine how much of the initial aluminum was converted to alumina, a comparison of initial and final masses of aluminum is made. It is assumed that the aluminum makes up 80 % mol of the sample. Multiplying the final mass of the deposit by the mole fraction of aluminum and dividing by the molecular weight of aluminum yields the mass of aluminum in the deposit.

Table 4. Total aluminum recovered

Test ID	Propellant Diameter [in]	Total Deposit Recovered [g]	Deposit w/o Al_2O_3 [g]	Initial Mass of Al [g]	Total Aluminum Recovered [%]
M-5	5	121	96.8	187.7	52
M-6	5	133	106.4	187.7	57
M-7	12	1591.7	1273.36	2604.2	49
M-8	12	1717.4	1373.92	2604.2	53
M-9	18	3132.6	2506.08	5724.4	44
M-10	18	3175	2540	5724.4	44
M-12	6	491.8	393.44	636.0	62
M-14	12	1613.3	1290.64	2604.2	50
M-16	18	2521.8	2017.44	5724.4	35

Figure 24 shows the relationship of the aluminum recovered and the propellant diameter. Data for tests M-5R, M-11, M-13, and M-15 were not provided.

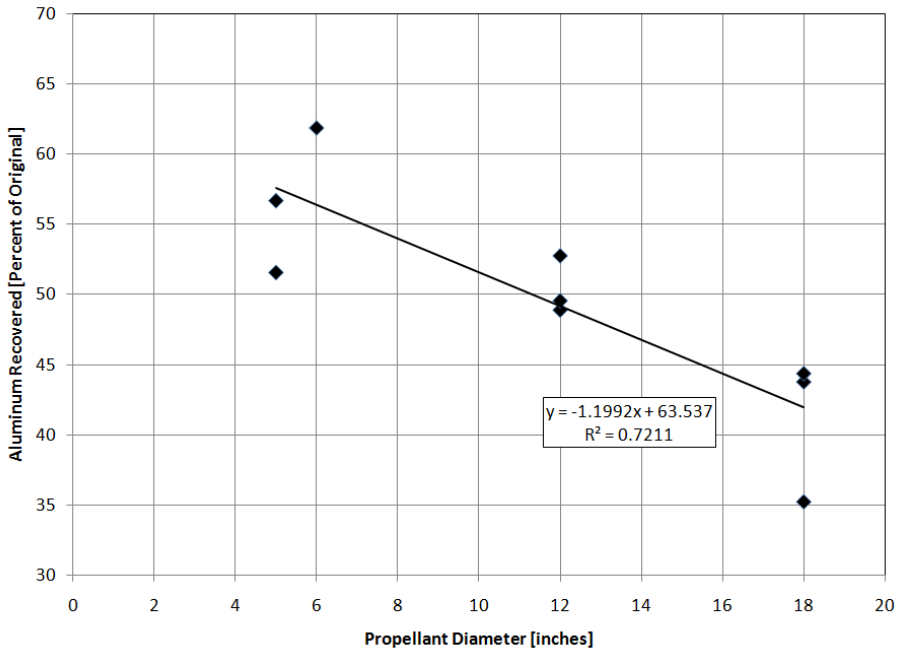

Figure 24. Recovered aluminum vs. propellant diameter

Conclusions

The effects of molten/oxidized aluminum in a solid propellant fire burning in an accident condition are difficult to quantify as the high heat of combustion of aluminum and aluminum particle impingement/deposition to target objects are complicated and not fully understood. The series of test performed in this report was designed to investigate the effects of molten/oxidized aluminum powder impingement/deposition on stainless steel substrates. A commercially available flame spray torch and powder hopper has been used to expose stainless steel substrates to a variety of conditions in an attempt to substantially degrade the substrate. SEM and EDS have been used to analyze the resulting amalgamation of aluminum and stainless steel. Aluminum particle penetration was observed and the resulting boundary layers were very sharp implying that the aluminum is unable to diffuse deep into the substrate. This implies that there is not necessarily a seriously degradation of stainless steel objects in the event of exposure to a solid propellant fire. However, this should not be taken to mean that stainless steel objects will survive a solid propellant fire as the temperature produced by the fire itself tends to cause significant degradation to the substrates. And if the aluminum ignites, then the additional heat release may result in more significant damage. SEM and EDS also illustrated that the aluminum powder was not oxidized by torch conditions. However, thermocouple data from the series of test show that significant increases in temperature occur when aluminum powder is introduced to the flame spray.

It is clear from Figure 24 that there is a strong relationship between the diameter of the propellant and the amount of aluminum that is be recovered. It is assumed any aluminum not recovered was converted to Al_2O_3 and lost in the heated plume. As the plume is the most likely loss of "stuff" that could be deposited, it would appear that the larger diameter propellant is able to convert more aluminum to alumina which is then carried away by the plume. This implicitly implies the larger diameter propellants are producing higher temperatures which facilitate the conversion of aluminum to alumina.

References

1. Kitahara, S., Hasui, A., *A Study of the Bonding Mechanism of Sprayed Coatings,* Journal of Vacuum Science Technology, Vol 11, No. 4, July/Aug 1874.
2. McPherson, R., *The Relationship between the Mechanism of Formation, Microstructure and Properties of Plasma-Sprayed Coatings,* Thin Solid Films, Vol 83, 1981, pp 297-310.
3. Urrea, D.A., Cates, J.W., Hall, A.C., Neiser, R.A., Smith, M.F., Hirschfeld, D.A., Proccedings of the 2006 International Thermal Spray Conference, May 2006.
4. Wikipedia contributors, "Stainless steel," *Wikipedia, The Free Encyclopedia,* http://en.wikipedia.org/w/index.php?title=Stainless_steel&oldid=229798875 (accessed August 6, 2008).
5. White, R., "Thermal Analysis of Aluminum Particle Combustion in a Simulated Solid Propellant Flame," A Thesis in Mechanical Engineering, Texas Tech University, Lubbock, Texas, May 2006.